Theoretical study of the influence of intense femtosecond laser field on the evolution of the wave packet and the population of NaRb molecule*

Ma Ning(马 宁), Wang Mei-Shan(王美山)†, Yang Chuan-Lu(杨传路), Ma Xiao-Guang(马晓光), and Wang De-Hua(王德华)

School of Physics and Electronic Engineering, Ludong University, Yantai 264025, *China*

(Received 13 July 2009; revised manuscript received 11 August 2009)

Employing the two-state model and the time-dependent wave packet method, we have investigated the influences of the parameters of the intense femtosecond laser field on the evolution of the wave packet, as well as the population of ground and double-minimum electronic states of the NaRb molecule. For the different laser wavelengths, the evolution of the wave packet of $6^1\Sigma^+$ state with time and internuclear distance is different, and the different laser intensity brings different influences on the population of the electronic states of the NaRb molecule. One can control the evolutions of wave packet and the population in each state by varying the laser parameters appropriately, which will be a benefit for the light manipulation of atomic and molecular processes.

Keywords: intense femtosecond laser field, time-dependent wave packet method, wave packet, population

PACC: 3380, 3390, 8240J

1. Introduction

In recent years, with the rapid development of ultrashort and ultrastrong laser pulse techniques, the light–matter interaction (LMI) has been demonstrated experimentally and studied theoretically.[1−3] An excellent review on the LMI is given in Ref. [4] and the references therein. When molecules are subjected to an intense laser field, many interesting phenomena have been observed, such as above-threshold ionization,[5−7] bond-hardening,[8] bond-softening,[9] ac-Stark shift,[10,11] Rabi oscillation,[12] etc.

Many alkali metal dimers have double-minimum potential states, such as $2^1\Sigma_u^+$ state of Na_2, $6^1\Sigma^+$ state of NaK , $6^1\Sigma^+$ state of NaRb, and so on.[13−18] Meier *et al.*[13] studied the electron kinetic energy distribution obtained from femtosecond pump/probe ionization of Na_2, which reflects details of the vibrational dynamics. And later, Assion *et al.*[14] mapped the molecular dynamics of Na_2, employing the kinetic energy time-of-flight mass spectroscopy in combination with the femtosecond pump-probe and molecular beam techniques. Yu *et al.*[15] reported the femtosecond pump-probe photoelectron spectra and the wave packet dynamics of the double-minimum potential $6^1\Sigma^+$ state of NaK in intense femtosecond laser field, using the time-dependent wave packet method. Korek *et al.*[16] calculated the potential energy over a wide range of internuclear distances for the 28 lowest electronic states of LiRb and NaRb molecules, using an *ab initio* method based on non-empirical pseudopotentials, parametrized l-dependent polarization potentials and full valence configuration interaction calculations. Docenko *et al.*[17] studied the potential energy of the ground state $X^1\Sigma^+$ of NaRb by the Fourier-transform spectroscopy, and an accurate potential energy curve was derived from more than 8800 transitions in isotopomers $^{23}Na^{85}Rb$ and $^{23}Na^{87}Rb$. Kortyka *et al.*[18] studied the double-minimum $6^1\Sigma^+$ state of NaRb, employing the polarization labeling spectroscopy technique.

To the best of our knowledge, the potential energy curves of the ground state $X^1\Sigma^+$ and the double-minimum state $6^1\Sigma^+$ of NaRb were studied in detail, but the wave packet dynamics of $6^1\Sigma^+$ state of NaRb in intense femtosecond laser field has not yet been investigated theoretically.

This paper is organized as follows: In Section 2, the theoretical model is introduced and the time-dependent Schrödinger equation is solved using the

*Project supported by the National Natural Science Foundation of China (Grant Nos. 10674114 and 10604045).

†Corresponding author. E-mail: mswang1971@163.com

© 2010 Chinese Physical Society and IOP Publishing Ltd

"split-operator Fourier-transform" method of wave packet propagation, and the expression of population in each electronic state is given. In Section 3, the evolution of the wave packet of $6^1\Sigma^+$ state of NaRb is discussed in detail for different laser wavelengths of the pump pulse. The influence of the laser intensity of the pump pulse on the population in both the ground and the double-minimum states of NaRb is also obtained. In Section 4, the main conclusions are summarized.

2. Theoretical treatment

In the calculation, the two-state model is employed: the ground state $X^1\Sigma^+$ and the double-minimum state $6^1\Sigma^+$ of the NaRb molecule. The relevant potential energy curves are shown in Fig. 1. The data of potential energy curves are taken from Refs. [16]–[18]. For convenience, the $X^1\Sigma^+$ and $6^1\Sigma^+$ states of NaRb are abbreviated to G and E, respectively.

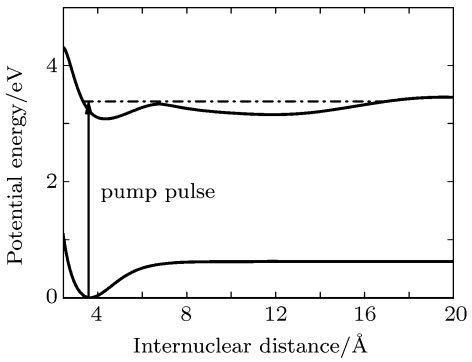


Fig. 1. Two-state model: a wave packet is pumped into the excited electronic state $6^1\Sigma^+$. The potential energy curves of electronic states $X^1\Sigma^+$ and $6^1\Sigma^+$ for the NaRb molecule are taken from Refs. [16]–[18] (1 Å=0.1 nm).

The rotational motion is ignored in our treatments because the heavy molecule does not rotate essentially on the femtosecond time scale.[13] Within the Born–Oppenheimer approximation, the time-dependent Schrödinger matrix equation can be written as

$$\mathrm{i}\hbar\frac{\partial}{\partial t}\begin{pmatrix}\Psi_{\mathrm{G}}(R,t)\\ \Psi_{\mathrm{E}}(R,t)\end{pmatrix}=\begin{pmatrix}H_{\mathrm{GG}} & H_{\mathrm{GE}}\\ H_{\mathrm{EG}} & H_{\mathrm{EE}}\end{pmatrix}\begin{pmatrix}\Psi_{\mathrm{G}}(R,t)\\ \Psi_{\mathrm{E}}(R,t)\end{pmatrix}, \tag{1}$$

where $\Psi_{\mathrm{G}}(R,t)$ and $\Psi_{\mathrm{E}}(R,t)$ represent the time-dependent nuclear wavefunctions for G and E, respectively. H_{ii} (i=G, E) and $H_{i,j}$ (i,j=G, E) are the diagonal elements and the off-diagonal elements, respectively. The diagonal elements can be expressed as

$$H_{ii}=-\frac{\hbar^2}{2m}\frac{\partial^2}{\partial R^2}I+V_{ii}(R),\quad (i=\mathrm{G},\mathrm{E}), \tag{2}$$

where m is the reduced mass of NaRb molecule, R the internuclear distance, I the identity matrix, and $V_{ii}(R)$ are the potential matrix elements of the molecule in absence of laser field.

The off-diagonal elements of the Hamiltonian can be expressed as

$$H_{ij}=H_{ji}=W_{ij}=\mu_{ij}E(t),\quad (i,j=\mathrm{G},\mathrm{E}), \tag{3}$$

where μ_{ij} is the transition dipole moment, which is assumed to be a constant because of its little dependence on the nuclear distance interested in our calculation. $E(t)$ is the electric field of the laser pulse given by

$$\boldsymbol{E}(t)=Ef(t)\cos[\omega(t-t_0)]\,\boldsymbol{e}, \tag{4}$$

where E is the amplitude of the electric field of the femtosecond laser pulse, ω the angular frequency, t_0 the centre time of the pulse, $\boldsymbol{e}$ the polarization vector. In the calculation, the polarization of the electric field is parallel to the nuclear axis.

The envelope shape $f(t)$ of the laser pulse with the Gaussian function is expressed as

$$f(t)=\exp\left(-(4\ln 2.0)(t-t_0)^2/\tau^2\right), \tag{5}$$

where τ is the full width at half maximum (FWHM) of the laser pulse. The above time-dependent Schrödinger matrix equation can be solved by the split-operator Fourier-transform method.[19–22] Within the second-order approximation, the evolution of the wave packets with time can be expressed as

$$\Psi(R,t_0+\Delta t)\approx\left[U_T^{1/2}(R,t_0)\,U_V U_T^{1/2}(R,t_0)\right]\times\Psi(R,t_0), \tag{6}$$

where $\Psi(R,t_0)$ is the wave packet at initial time t_0, which is usually chosen as the wavefunction of the ground vibrational state of the ground electronic state $X^1\Sigma^+$ of NaRb, Δt is the time interval, and U_T and U_V denote the kinetic and potential energy evolution operators, respectively. The kinetic energy evolution operator is given by

$$U_T=\exp\left[-\frac{\mathrm{i}\Delta t}{\hbar}T_R\right]=F^{-1}\exp\left[-\frac{\mathrm{i}\hbar k^2\Delta t}{2\mu}\right]F, \tag{7}$$

where F denotes the Fourier transform

$$F[f]=\frac{1}{\sqrt{2\pi}}\int_{-\infty}^{+\infty}\mathrm{d}R'\mathrm{e}^{\mathrm{i}kR'}f(R'). \tag{8}$$

The potential evolution operator can be expressed as[20,21]

$$U_V = \exp\left[-\frac{\mathrm{i}}{\hbar}V\Delta t\right] = M\exp\left[-\frac{\mathrm{i}}{\hbar}M^T V M\Delta t\right]M^{\mathrm{T}}$$
$$= M\begin{pmatrix}\exp\left(-\mathrm{i}\,\lambda_1\Delta t/\hbar\right) & 0\\ 0 & \exp\left(-\mathrm{i}\,\lambda_2\Delta t/\hbar\right)\end{pmatrix}M^{\mathrm{T}}, \tag{9}$$

where V is the potential matrix, which can be written as

$$V(R,t) = \begin{pmatrix}V_{\mathrm{GG}} & \mu E(t)\\ \mu E(t) & V_{\mathrm{EE}}\end{pmatrix}, \tag{10}$$

and M denotes the matrix which diagonalizes $V(R,t)$, the superscript T represents the transpose of the matrix, and λ_1 and λ_2 are the eigenvalues of the matrix V.

After propagating n steps, the wavefunction can be written as

$$\Psi(R,t_0+n\Delta t) = \left[\prod_{k=0}^{n-1}U_T^{1/2}(R,t_0+k\Delta t)\,U_V U_T^{1/2}(R,t_0+k\Delta t)\right]\Psi(R,t_0). \tag{11}$$

Once the wave function $\Psi(R,t)$ is determined, the population in each electronic state can be written as

$$P_i(t) = \int \mathrm{d}R\,|\Psi_i(R,t)|^2, \quad i = \mathrm{G},\mathrm{E}. \tag{12}$$

3. Results and discussion

3.1. Influence of the laser wavelength on the evolution of the wave packet of $6^1\Sigma^+$ state

The electronic state $6^1\Sigma^+$ of NaRb is a double-minimum potential state. The minima of the inner and outer potential wells lie at $R = 4.34018$ and $R = 1188856$ Å (1 Å=0.1 nm), respectively, and their corresponding potential energies are $U(R) = 3.08129$ eV and 315539 eV. Whereas the barrier height E_{b} is 3.34067 eV, which lies at $R = 6.71554$ Å, and the energy of the ground vibrational state of the ground electronic state $\mathrm{X}^1\Sigma^+$ is $E_{00} = 6.6\times10^{-3}$ eV. The intensity and the FWHM of the pump pulse are taken as 9.0×10^{13} W/cm^2 and $\tau = 80$ fs, respectively. In the following, three cases will be discussed separately: $E_\alpha < E_{\mathrm{b}}$, $E_\alpha \approx E_{\mathrm{b}}$ and $E_\alpha > E_{\mathrm{b}}$ ($E_{00}+h\omega = E_\alpha$). Figure 2 shows the evolution of the wave packet with time and internuclear distance when $E_\alpha < E_{\mathrm{b}}$, and the corresponding pump wavelength $\lambda = 403$ nm. Two characteristics can be observed clearly in Fig. 2. First, the motion of almost all the wave packet takes place in the inner potential well and is restricted by the classical turning points, which belongs to the mean energy of the wave packet. The oscillating period of the wave packet is about 250 fs. Secondly, a small part of the wave packet passes through the barrier and moves away towards larger distance. That is because the ultrashort laser pulse has a broad spectral distribution, some bound states with energies above the barrier are excited with a small probability.[13] The pump wavelength is $\lambda = 372$ nm for the case $E_\alpha \approx E_{\mathrm{b}}$, and the results are shown in Fig. 3. A pronounced character can be observed clearly that the wave packet splits into two parts in the barrier region. This can be interpreted by the fact that the vibrational states below and above the barrier are excited with comparable probabilities.[13] And, one can see that part of the wave packet moves into the outer well and is reflected and then moves back inwards at the outer turning point (at about 18 Å). Its oscillating period is about 1600 fs. The other part of the wave packet still remains in the inner potential well and its oscillating period is about 600 fs. If the peak energy of the pump pulse plus the energy of the initial state is increased to a value larger than the barrier height ($E_\alpha > E_{\mathrm{b}}$), e.g. $\lambda = 350$ nm , the created wave packet will pass through the barrier region and only a small part is reflected as illustrated in Fig. 4. The wave packet moves towards the larger internuclear distances and is reflected at the outer turning point and then moves back inwards hereafter.

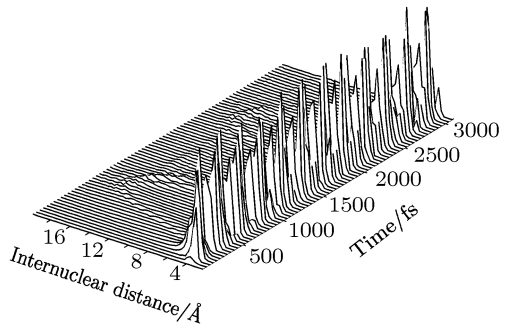


Fig. 2. The evolution of the wave packet of double-minimum potential state $6^1\Sigma^+$ with time and internuclear distance for $E_\alpha < E_\mathrm{b}$ and $\lambda = 403$ nm.

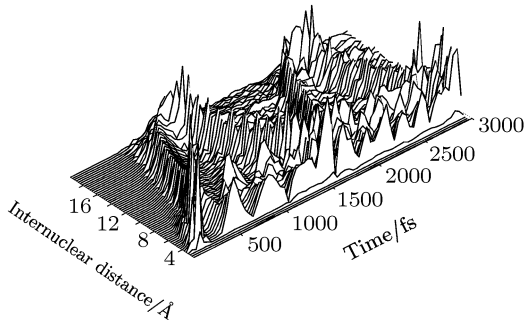


Fig. 3. The evolution of the wave packet of double-minimum potential state $6^1\Sigma^+$ with time and internuclear distance for $E_\alpha \approx E_\mathrm{b}$ and $\lambda = 372$ nm.

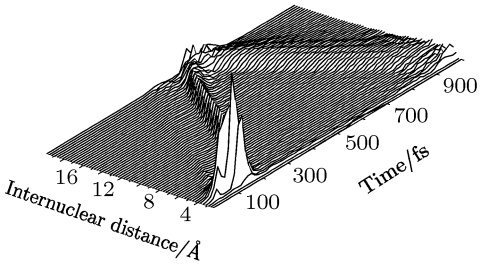


Fig. 4. The evolution of the wave packet of double-minimum potential state $6^1\Sigma^+$ with time and internuclear distance for $E_\alpha > E_\mathrm{b}$ and $\lambda = 350$ nm.

3.2. Influence of the laser intensity on the population of the electronic states

In order to investigate the influence of the laser intensity on population, the intensity is varied from 1.0×10^{13} W/cm^2 to 9.0×10^{15} W/cm^2. All the laser parameters are fixed except for the laser intensity. In the calculation, the pulse width $\tau = 80$ fs, the centre wavelength $\lambda = 403$ nm. Figure 5 shows the changes of population with the evolution time for different laser intensities. Figures 5(a)–5(d) correspond to those for the pulse intensities of 1.0×10^{13}, 3.0×10^{13}, 6.0×10^{13} and 9.0×10^{13} W/cm^2, respectively. It can be seen that when the pulse is present, the population in each state will take the form of oscillation, which is often called Rabi oscillation.[23] Three characters can be seen from Fig. 5. First, the total populations of the ground state G and the double-minimum state E of the NaRb are equal to 1. Secondly, for lower laser intensity, the population of G state is bigger than that of E state. With the increase of the laser intensity, the population in G state decreases while that in E state increases. Finally, the phenomenon of Rabi oscillation can be observed clearly as documented in Figs. 5(c) and 5(d). For the laser intensity of the order of magnitude of 10^{14} W/cm^2, the calculation results are shown in Fig. 6. Figures 6(a)–6(d) correspond to those for the pulse intensities of 1.0×10^{14}, 3.0×10^{14}, 5.0×10^{14}, and 6.0×10^{14} W/cm^2, respectively. Four characters can be seen from Fig. 6. First, most of the populations are transferred from G state to E state with the increase of the laser intensity, resulting in the decrease of population in G state and the increase in E state. Secondly, when the pulse is turned off at 230 fs, the Rabi oscillation will disappear simultaneously, but each state will still be occupied and unchangeable in the time ranging from 230 fs to 600 fs. Thirdly, the frequency of Rabi oscillation increases with the increase of the laser intensity, which is consistent with the results given in Refs. [24] and [25]. This phenomenon can be rationalized by the formula $P(t) = (E_0^2/\hbar^2\Omega_\mathrm{R}^2)\sin^2\left(\frac{1}{2}\Omega_\mathrm{R}t\right)$,[23] where $\Omega_\mathrm{R} = \left[(\omega_\mathrm{L}-\omega_0)^2 + E_0^2/\hbar^2\right]^{1/2}$ is the Rabi frequency; ω_0, E_0 and ω_L is the resonance frequency for the related transition, the amplitude of the electric field and the centre frequency of the pulse, respectively. According to the formula of the Rabi frequency and the fact that E_0 is proportional to the square root of the laser intensity, increasing E_0 will result in the increase of Rabi frequency Ω_R, so it is easy to understand the relationship between the laser intensity and the Rabi frequency. Finally, the residual population in each state is different when the laser pulse is turned off. This can be interpreted by the fact that the frequencies of the Rabi oscillation are different with the change of the laser intensity, which leads to the different population left over in each state. When the laser intensity increases to 3.0×10^{15} W/cm^2, one can clearly see the high frequency oscillation riding on the top of the Rabi oscillation, as presented in Fig. 7. It can be attributed to the nonrotating wave component in strong laser fields,[3] because we have not taken the rotating wave approximation into account in our calculation.[26]

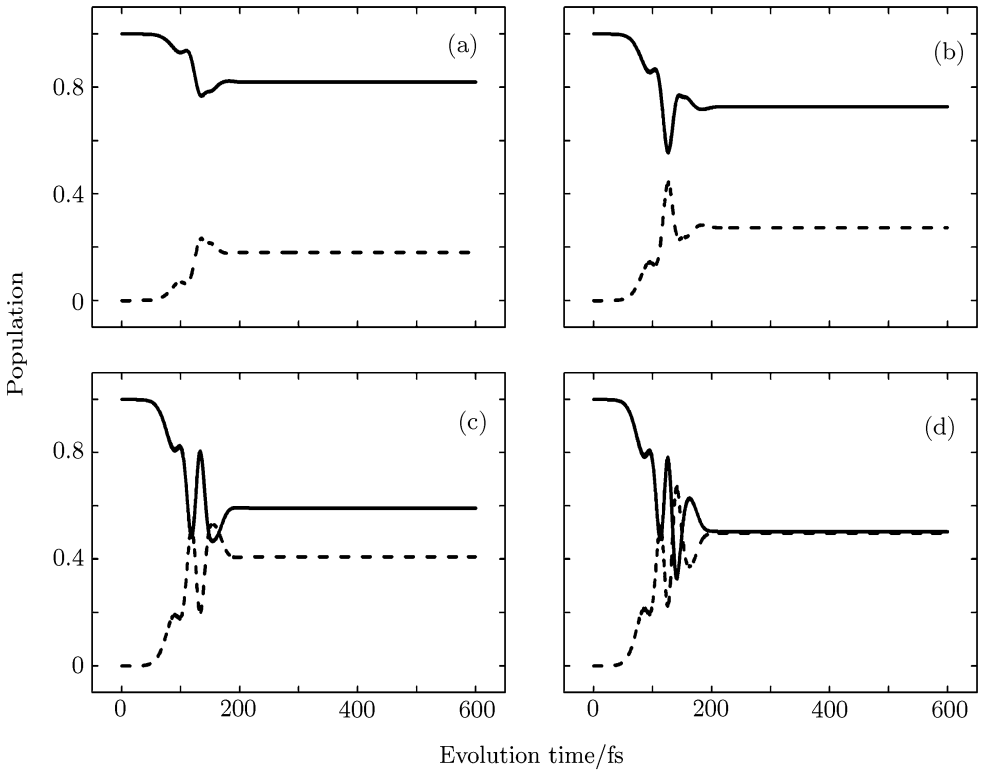


Fig. 5. Time evolution of the ground state (solid line) and the double-minimum state (dashed line) populations for different laser intensities, in unit of W/cm^2: (a) 1.0×10^{13}, (b) 3.0×10^{13} (c) 6.0×10^{13}, and (d) 9.0×10^{13}.

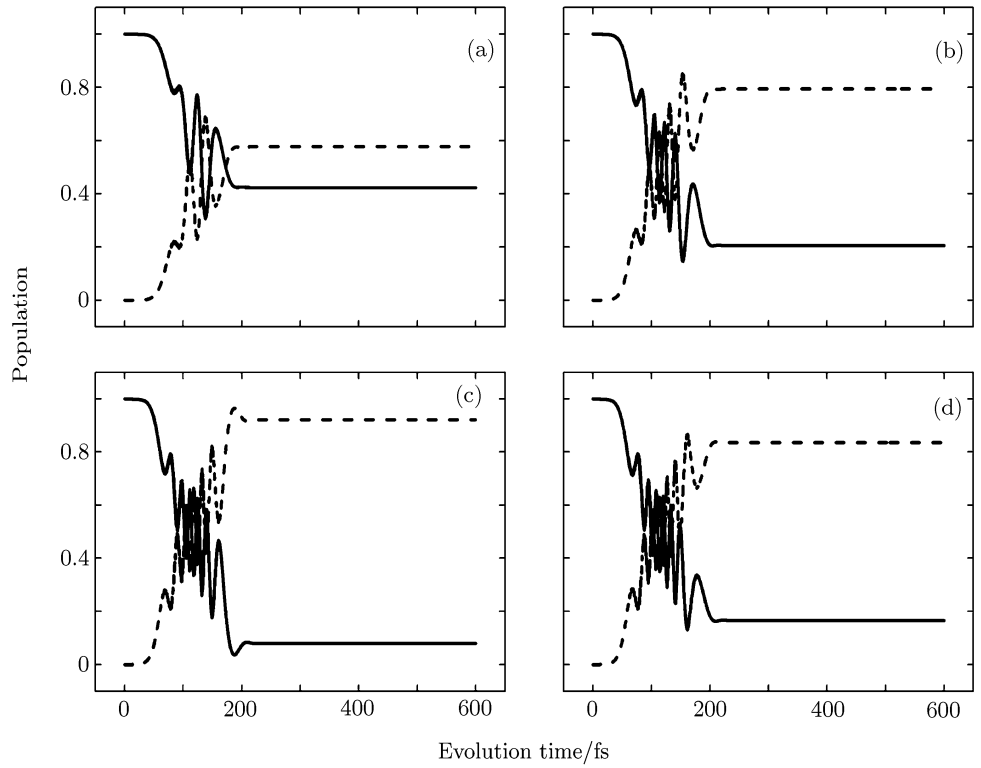


Fig. 6. Time evolution of the ground state (solid line) and the double-minimum state (dashed line) populations for different laser intensities, in unit of W/cm^2: (a) 1.0×10^{14}, (b) 3.0×10^{14}, (c) 5.0×10^{14} and (d) 6.0×10^{14}.

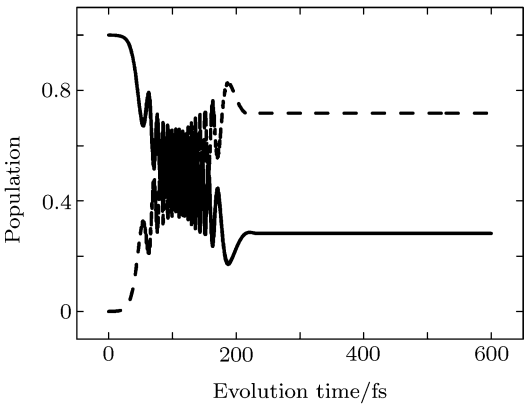


Fig. 7. Time evolution of the ground state (solid line) and the double-minimum state (dashed line) populations for laser intensity 3.0×10^{15} W/cm^2.

4. Conclusions

In this paper, we have studied theoretically the influence of laser wavelength on the evolution of wave packet of the double-minimum potential state $6^1\Sigma^+$ and the influence of laser intensity on the population of $X^1\Sigma^+$ and $6^1\Sigma^+$ states of the NaRb molecule in an intense femtosecond laser field, using the two-state model and the time-dependent wave packet method. For different laser wavelengths, the evolution of the wave packet of $6^1\Sigma^+$ state of the NaRb molecule with time and internuclear distance is different. Furthermore, the wave packet will split into two parts in the barrier region when the peak energy of the pump pulse plus the energy of the initial state equals the barrier energy. The different laser intensity has a different influence on the population of the electronic states of NaRb molecule. Rabi oscillation is enhanced with the proper laser intensity and the high frequency oscillation riding on the top of the Rabi oscillation when the laser intensity is higher. The calculated results indicate that one can control the evolutions of wave packet and the population in each state by varying the laser parameters, such as the wavelength and the intensity of the laser pulse, which will be a benefit for the light manipulation of atomic and molecular processes.

Acknowledgement

The authors are indebted to Prof. Han Ke-Li for providing the code used in our calculation. All calculations for the present study were carried out at the Dawning 4000A Computer Centre of Ludong University.

References

[1] Wunderlich C, Kobler E, Figger H and Hänsch T W 1997 *Phys. Rev. Lett.* **78** 2333
[2] Walker B C, Tóth C, Fittinghoff D N, Guo T, Kim D E, Rose-Petruck C, Squier J A, Yamakawa K, Wilson K R and Barty C P J 1999 *Opt. Express* **5** 196
[3] Garraway B M and Suominen K A 1998 *Phys. Rev. Lett.* **80** 932
[4] Pukhov A 2003 *Rep. Prog. Phys.* **66** 47
[5] Zavriyev A, Bucksbaum P H, Muller H G and Schumacher D W 1990 *Phys. Rev.* A **42** 5500
[6] Giusti-Suzor A, He X, Atabek O and Mies F H 1990 *Phys. Rev. Lett.* **64** 515
[7] Grasbon F, Paulus G G, Walther H, Villoresi P, Sansone G, Stagira S, Nisoli M and De Silvestri S 2003 *Phys. Rev. Lett.* **91** 173003
[8] Frasinski L J, Posthumus J H, Plumridge J, Coding K, Taday P F and Langley A J 1999 *Phys. Rev. Lett.* **83** 3625
[9] Bucksbaum P H, Zavriyev A, Muller H G and Schumacher D W 1990 *Phys. Rev. Lett.* **64** 1883
[10] Sun Z G, Liu H P, Lou N Q and Cong S L 2003 *Chem. Phys. Lett.* **369** 374
[11] Stapelfeldt H, Sakai H, Constant E and Corkum P B 1997 *Phys. Rev.Lett.* **79** 2787
[12] Magnier S, Persico M and Rahman N 1999 *Phys. Rev. Lett.* **83** 2159
[13] Meier C and Engel V 1994 *J. Chem. Phys.* **101** 2673
[14] Assion A, Baumert T, Geisler M, Seyfried V and Gerber G 1998 *Eur. Phys. J.* D **4** 145
[15] Yu J, Wang S M, Yuan K J and Cong S L 2006 *Chin. Phys.* **15** 1996
[16] Korek M, Allouche A R, Kobeissi M, Chaalan A, Dagher M, Fakherddin K and Aubert-Frécon M 2000 *Chem. Phys.* **256** 1
[17] Docenko O, Tamanis M, Ferber R, Pashov A, Knöckel H and Tiemann E 2004 *Phys. Rev.* A **69** 042503
[18] Kortyka P, Jastrzebski W and Kowalczyk P 2005 *Chem. Phys. Lett.* **404** 323
[19] Feit M D, Fleck Jr J A and Sreiger A 1982 *J. Comput. Phys.* **47** 412
[20] Chu T S, Zhang Y and Han K L 2006 *Int. Rev. Phys. Chem.* **25** 201
[21] Xie T X, Zhang Y, Zhao M Y and Han K L 2003 *Phys. Chem. Chem. Phys.* **5** 2034
[22] Hu J, Han K L and He G Z 2005 *Phys. Rev. Lett.* **95** 123001
[23] Knight P L and Milonni P W 1980 *Phys. Rep.* **66** 21
[24] Meng Q T, Yang G H and Han K L 2003 *Int. J. Quantum Chem.* **95** 30
[25] Meng Q T, Liu X G, Zhang Q G and Han K L 2005 *Chem. Phys.* **316** 93
[26] Brown A, Meath W J and Tran P 2000 *Phys. Rev.* A **63** 013403